Investigation of the influence of the front end clearance on the parameters of a centrifugal pump with an open type impeller

S Kalinkin[1] and A Petrov[1,2]

[1]Bauman Moscow State Technical University

[2]E-mail: alexeypetrov@bmstu.ru

Abstract: The paper considers the influence of the size of the front end gap between the impeller and the housing on the energy performance of the pump, selects the parameters, compiles a mathematical model used in hydrodynamic modeling, presents the results of the study, draws conclusions about the influence of the size of the front gap between impeller and housing on efficiency and pump head. A comparison is made of the dimensionless pump characteristics obtained by the methods of hydrodynamic modeling with experimental dependences.

Introduction

In the case of the development of centrifugal pumps with a low speed coefficient, the question often arises of choosing the type of impeller [1]. The impeller can be closed, half open and open type, each of which has its advantages and disadvantages. So the open type impeller consumes much less power when working at high viscosity [2] relative to other types, does not have a front gap seal, which allows pumping contaminated liquid [3–9]. However, due to the lack of a driven disk, it is impossible to accurately calculate volumetric losses, since the fluid flow in the gaps between the impeller and the walls of the casing is part of the working process of the impeller [10–12]. It is also worth noting that currently there is not enough literature for the design of impellers with low and ultra-low speed coefficient, and theoretical formulas give large errors. Therefore, at this stage, it is necessary to make sure that the calculations of the complex flow in the open impeller, including the end gap region, can be performed by numerical simulation methods and to verify the obtained calculated dependences by comparing them with experimental data.

Methods

The method of numerical simulation is based on the solution of discrete analogues of the basic equations of hydrodynamics. In the case of the selected model of an incompressible fluid ($\rho = const$), this is:

The continuity equation of a liquid medium [1]:

$$\frac{\partial \overline{u_x}}{\partial x} + \frac{\partial \overline{u_y}}{\partial y} + \frac{\partial \overline{u_z}}{\partial z} = 0,$$

where $\overline{u_i}$ — time-averaged projections of fluid velocities on the corresponding axes;

The equation of change in momentum [7]

In such a simulation, there is a flow region that rotates with the rotor - this is the flowing part of the impeller. The flow equation for a given region is written in terms of relative motion [4], so the equation of change in momentum is as follows:

$$\rho\left(\frac{\partial \overline{W_i}}{\partial t}+u_j\frac{\partial \overline{W_i}}{\partial x_j}\right)=-\frac{\partial \overline{p}}{\partial x_i}+\frac{\partial}{\partial x_i}\left(T_{ij}^{(\nu)}-\rho W_i W_j\right)+F_i+F_\kappa,$$

where $\overline{W_i}$ — average speed: $\overline{W}=\overline{V}-\overline{u}$ — ratio of relative, absolute and transfer speeds;

$\overline{p}$ — averaged pressure;

$T_{ij}^{(\nu)}=2\mu s_{ij}$ —viscous stress tensor for incompressible fluid;

$s_{ij}=\frac{1}{2}\left(\frac{\partial \overline{W_i}}{\partial x_j}+\frac{\partial \overline{W_j}}{\partial x_i}\right)$ — strain rate tensor;

$\rho W_i W_j$ — Reynolds stresses;

$F_i=\rho\omega^2 r$ —inertia force;

$F_\kappa=2\omega W_{xy}$ —cariolis stress.

The Reynolds system of equations [1] is open due to the presence of unknown Reynolds stresses. System closure is performed using the k-ωSST turbulence model [5]. This model combines k-ω and k-ε models: the first is used in the near-wall region, the second in the central part of the flow.

This model includes two equations of transport of turbulence parameters [12]:

1. The equation of transfer of kinetic energy of turbulence

$$\frac{\partial k}{\partial t}+\overline{u_j}\frac{\partial k}{\partial x_j}=P_k-\beta\cdot k\omega+\frac{\partial}{\partial x_i}\left[\left(\nu+\sigma_k\nu_T\right)\frac{\partial k}{\partial x_j}\right],$$

where $k=\frac{1}{2}\left(u_x'^2+u_y'^2+u_z'^2\right)$ — kinetic energy of turbulence;

u_i' —pulsation of speed;

P_k —turbulence energy generation;

ω —relative turbulence dissipation rate;

ν_T —turbulent viscosity.

2. The equation of transport of the relative velocity of dissipation of turbulence energy:

$$\frac{\partial \omega}{\partial t}+\overline{u_j}\frac{\partial \omega}{\partial x_j}=\alpha S^2-\beta\omega^2+\frac{\partial}{\partial x_i}\left[\left(\nu+\sigma_\omega\nu_T\right)\frac{\partial \omega}{\partial x_j}\right]+2\left(1-F_j\right)\sigma_{\omega 2}\frac{1}{\omega}\frac{\partial k}{\partial x_j}\frac{\partial \omega}{\partial x_j}$$

Reynolds stresses in the equations of dynamics are based on the Boussinesq hypothesis:

$$\rho u_i u_j=2\mu_T\left[\frac{1}{2}\left(\frac{\partial u_i}{\partial x_j}+\frac{\partial u_j}{\partial x_i}\right)-\frac{1}{3}\frac{\partial u_k}{\partial x_k}\delta_{ij}\right]-\frac{2}{3}\rho k\delta_{ij},$$

where δ_{ij} —Kronecker symbol.

Using empirical closure coefficients of these equations [11], one can obtain a numerical solution of the turbulent fluid flow in the computational domain.

The impeller has been designed for the following parameters.:

$H=25m$ — pressure head,

$Q = 25\,m^3\,/\,h$ — flow rate,

$n = 2900\,rpm$ —rotation speed.

The drawing of the impeller under study is shown in Figure 1. The drawing shows the size δ_1 of the front axial clearance between the wheel and the casing wall, as well as the width b_2 of the impeller at the exit, along which dimensioning was carried out. The size δ_2 of the rear axial clearance between the wheel and the housing wall is fixed and equal to half the width b_2.
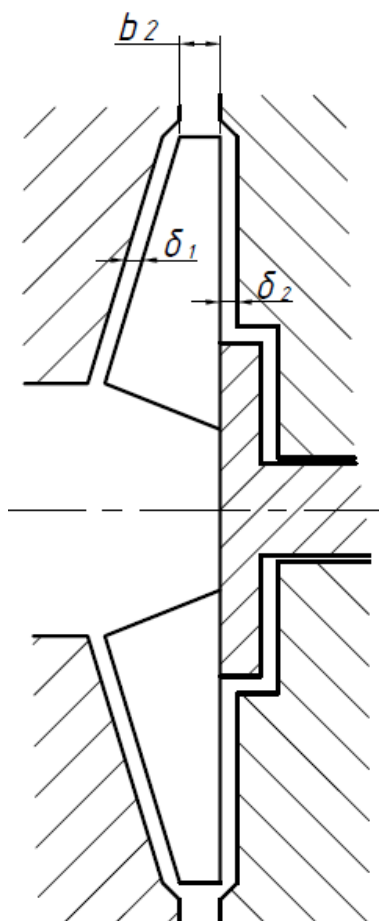

Figure 1. Impeller drawing

When modeling the fluid flow, it is necessary to break the flow geometry into cells, for which the equations given above [5] will be applied. For this, a model was chosen that generated polyhedral cells, as well as a model for constructing prismatic cells for modeling fluid flow near the wall [9]. A value of 5 mm was taken as the base size. The maximum and minimum cell sizes and the thickness of the boundary layer were specified as a percentage of the base size — 80%, 40%, and 24%, respectively. For the mesh in the impeller, the cell sizes are different from those specified for the entire model: the maximum cell size is 40%, the minimum cell size is 20%. The stretching of the prismatic layer occurs with a coefficient of 1.3. 5 layers have been created. At the exit from the spiral outlet, an extruder was created with a constant speed parameter in the normal direction [10]. The length of the extruder is 1 m, the number of layers is 500. It is necessary to equalize the flow at the output boundary [12] in order to reduce the influence of reverse currents, which significantly reduces the calculation accuracy near the boundary. An example of the generated grid is shown in Figure 2. To check the accuracy of the results, a calculation was performed with increased accuracy with the

following values of the main parameters: the base size is 2.5 mm, the maximum cell size is 50%, the minimum cell size is 20%, boundary layer thickness — 48%; for the impeller: the maximum cell size is 20%, the minimum cell size is 10%. The discrepancy between the results of a more accurate and simplified modeling is insignificant (less than 0.5%). Thus, all calculations were performed on simplified models to reduce the calculation time.
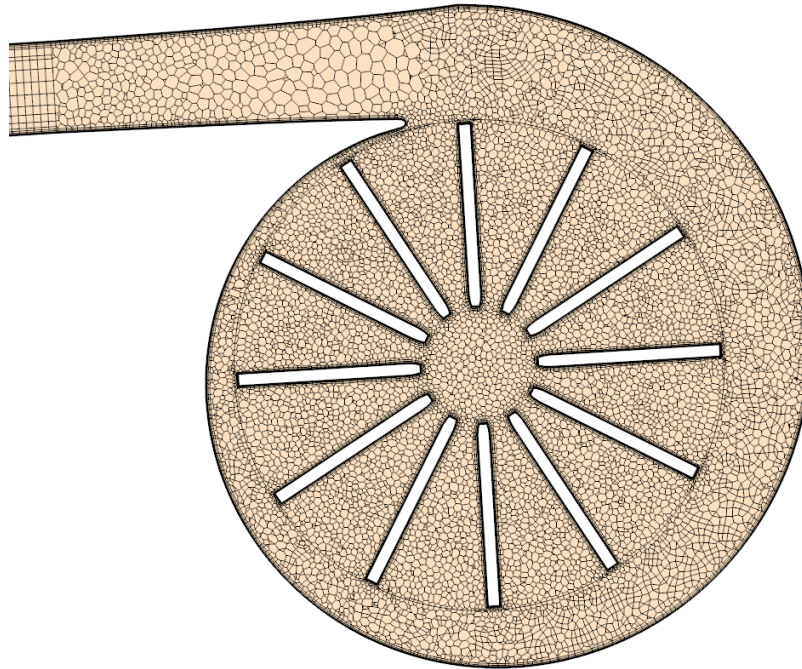

Figure 2. Impeller cross section

In this study, the value of only the front gap was changed, since the influence of the dimensions of the rear gap does not strongly affect the power characteristic [2]. The relative gap value is calculated by the formula

$$\Delta = \frac{\delta_1}{b_2}.$$

For the calculation, models with a relative gap Δ from 0.1 to 1.0 in increments of 0.1 were used. The correspondence between the numbers of the studied models and the values of the relative gap Δ are given in table 1.

Table 1

Model no.	1	2	3	4	5	6	7	8	9	10
Δ	0,1	0,2	0,3	0,4	0,5	0,6	0,7	0,8	0,9	1,0

Results

When simulating the flow, the following were determined: pressure at the inlet to the inlet and outlet of the spiral outlet, the moment at the impeller. After processing the results, the following values were obtained: the pressure created by the impeller, the moment on the impeller, and efficiency. The results are shown in table 2.

Table 2

Model no.	H, m	M, N·m	η
1	25,79	2,679	68,95
2	25,97	2,740	67,87
3	25,55	2,723	67,18
4	25,26	2,710	66,73
5	25,09	2,700	66,55
6	24,87	2,680	66,44
7	24,71	2,668	66,33
8	24,58	2,665	66,06
9	24,38	2,655	65,76
10	24,27	2,660	65,32

In [2], experimental results are presented. For comparison, the pressure was reduced to a dimensionless form by the formula

$$\bar{H} = \frac{H}{\left(D_2 \cdot n\right)^2} \, ,$$

and for efficiency the coefficient is used

$$k_\eta = \frac{\eta}{\eta_{max}} \, .$$

The obtained values are displayed on the graphs (Figure 4, 5) of the dependence of the dimensionless pressure and efficiency coefficient on the dimensionless axial clearance — $\bar{H}(\Delta)$ and $k_\eta(\Delta)$.

The dependences obtained by calculation were compared with the experimental data given in [2]. The results, recalculated in the same dimensionless quantities, are shown in Figures 4 and 5. Good convergence of the type of experimental and theoretical characteristics is visible. A certain deviation can be explained by a limited number of experimental points and a certain difference in the speed coefficients of the impeller, on which the experiments were performed, and the impeller investigated by hydrodynamic modeling methods, as well as by a small (for such pump parameters) absolute value of efficiency, which increases the "price" of its minimum deviation in absolute terms.
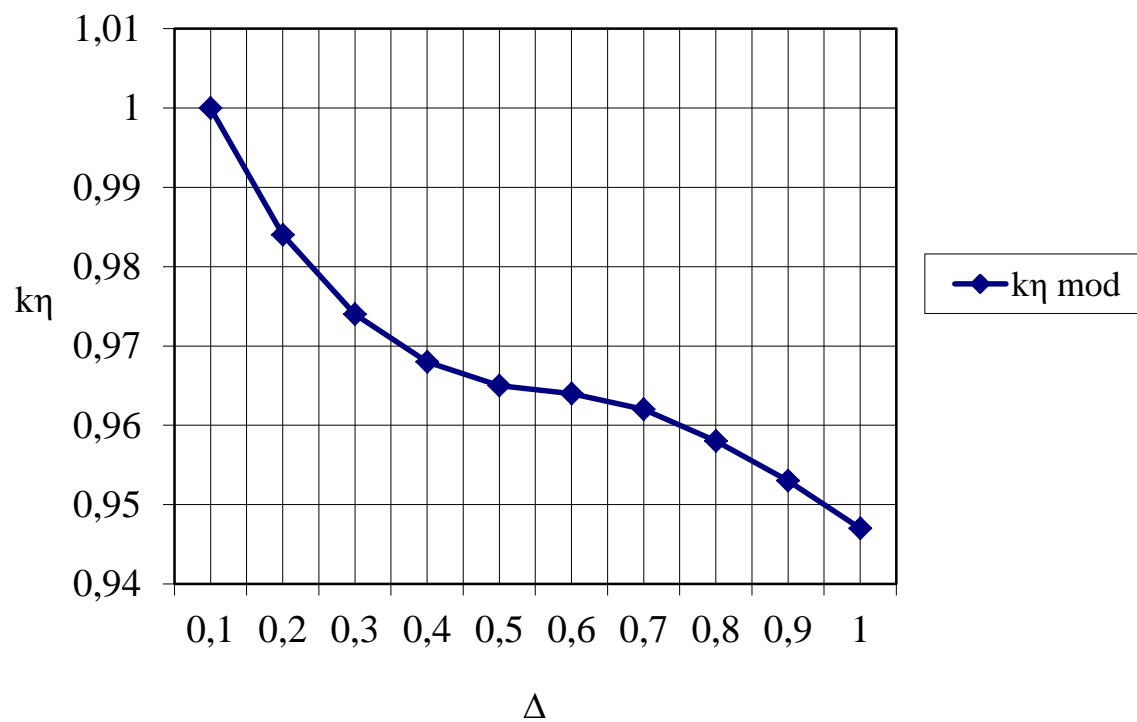
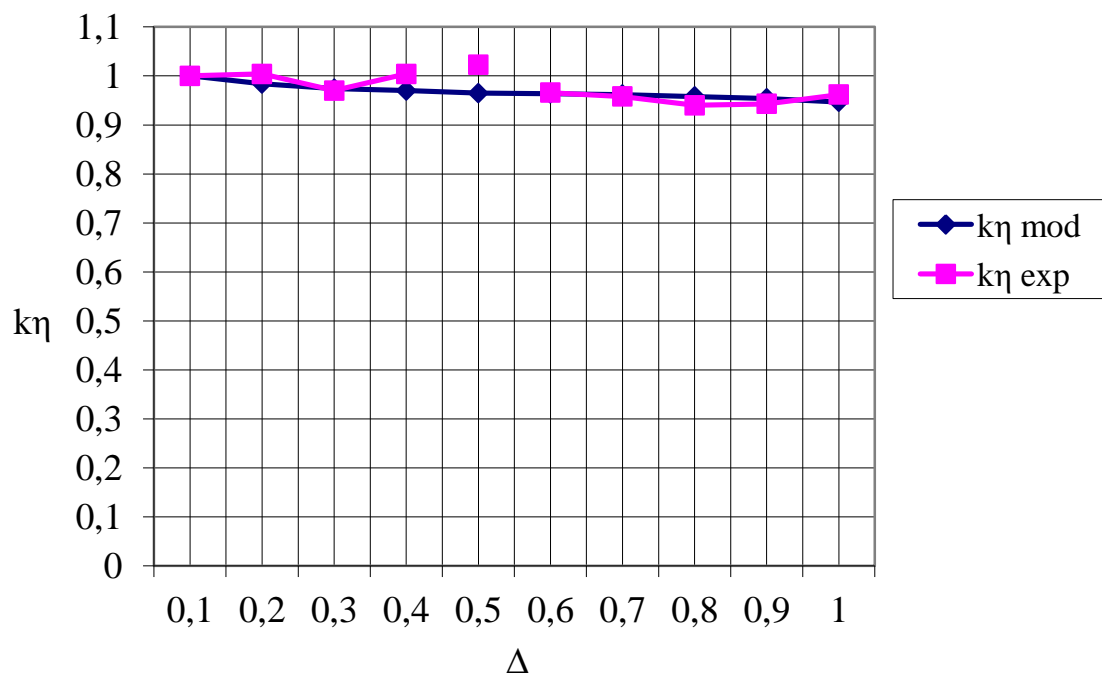**Figure 3.** Dependence graph $k_\eta(\Delta)$ obtained by hydrodynamic modeling
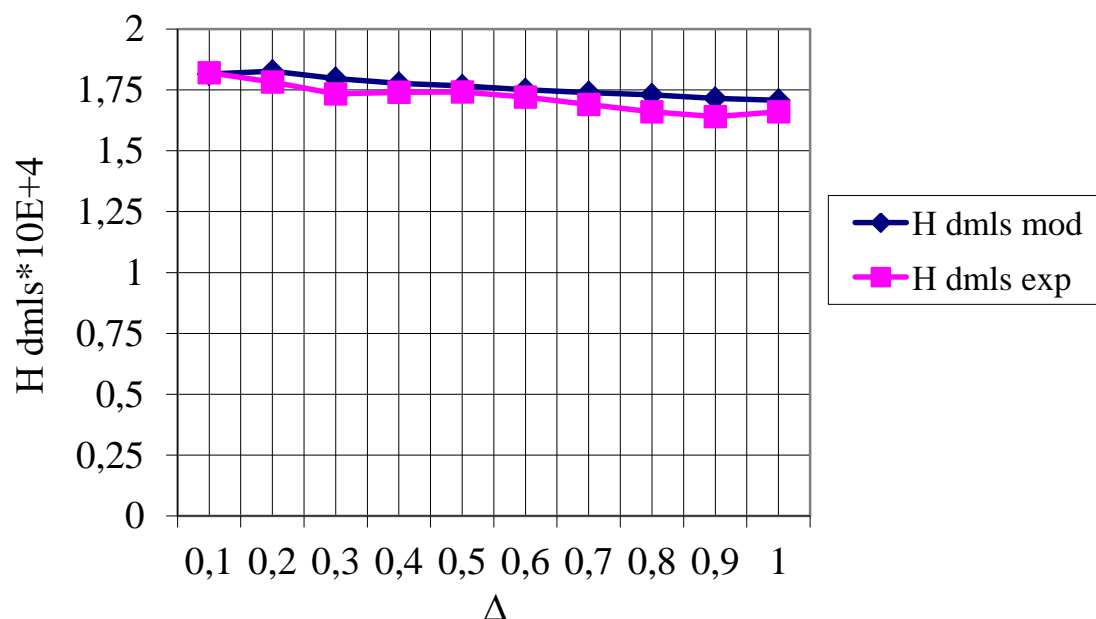

Figure 4. Dependency graph $k_\eta(\Delta)$

Figure 5. Dependency graph $\bar{H}(\Delta)$

Conclusion

1. Good convergence of the efficiency coefficient graphs was obtained, with the exception of one experimental value at $\Delta = 0,5$, which is explained by small values of efficiency, and therefore, a large influence of the error.

  2. The graph of the dimensionless pressure repeats the shape of the experimental curve, however, it has slightly larger values and does not completely coincide. Such a difference could arise due to a different slope of the pressure characteristic due to a different speed coefficient. This issue requires for there study.

  3. On the obtained efficiency graph, the area is clearly visible on which the change in the values of the function of the end gap is small. The presence of such a zone can save on ensuring the accuracy of manufacturing parts included in the dimensional chain, while maintaining a high value of efficiency.

References

[1]   Loitsyansky L.G. Fluid and Gas Mechanics — 4th ed. — M.: Publishing House "Science", 1973.
[2]   Matveev I.V., Petrov A.I. The study of the influence on the pressure characteristic of the pump of the front clearance between the open impeller and the housing. // 50 years kaf. GM: Thesis. Doc. MNTK — M., MPEI, 1996.— P. 87.
[3]   Petrov A.I. The effect of high viscosity of the working fluid on the parameters of ultra-low speed centrifugal pumps with open impellers. // Hydraulic Engineering. Present and future .: Abstract. Doc. MNTK — M., MSTU, 2004.— S. 50.A Petrov et al 2019 *IOP Conf. Ser.: Mater. Sci. Eng.* 492 012036
[4]   A Protopopov and D Bondareva 2019 *IOP Conf. Ser.: Mater. Sci. Eng.* 492 012002
[5]   A Protopopov and V Vigovskij 2019 *IOP Conf. Ser.: Mater. Sci. Eng.* 492 012003
[6]   K Dobrokhodov and APetrov 2019 *IOP Conf. Ser.: Mater. Sci. Eng.* 492 012016
[7]   N Egorkina and APetrov 2019 *IOP Conf. Ser.: Mater. Sci. Eng.* 492 012015
[8]   N Isaev 2019 *IOP Conf. Ser.: Mater. Sci. Eng.* 492 012026

[9]   T Valiev and APetrov 2019 *IOP Conf. Ser.: Mater. Sci. Eng.* 492 012038

[10] V Cheremushkin and V Lomakin 2019 *IOP Conf. Ser.: Mater. Sci. Eng.* 492 012039

[11] V Lomakin and O Bibik 2019 *IOP Conf. Ser.: Mater. Sci. Eng.* 492 012037

[12] V Lomakin et al 2019 *IOP Conf. Ser.: Mater. Sci. Eng.* 492 012012